

# Local Minimum of Elastic Potential Energy on Hemispherical Soft Fingertip

Takahiro Inoue and Shinichi Hirai

Department of Robotics, Ritsumeikan Univ.,  
1-1-1 Noji-Higashi, Kusatsu, Shiga 525-8577, Japan  
gr018026@se.ritsumei.ac.jp

**Abstract**— This paper proposes a new contact deformation model between a hemispherical soft fingertip and an object. First, we develop our proposed contact model, in which an elastic potential energy is formulated. Second, we show that the elastic potential energy due to the deformation of the soft fingertip is proportional to the cube of the maximum displacement of that fingertip. Also, it is firstly shown that the elastic force and the potential energy are functions of two variables: the maximum displacement and the orientation angle of the contact object. The most important point is that the potential energy of the fingertip have a local minimum when the object contacts with the soft fingertip keeping a vertical direction. Finally, we show that the local minimum of the elastic potential energy also appears in experiments.

**Index Terms**— Soft fingertip, Tactile sensor, Local minimum, Elastic force, Potential energy, Manipulation.

## I. INTRODUCTION

Human fingers have a characteristic of viscoelasticity and deform easily according to the shape of an grasped object. Furthermore, we can stably grasp and manipulate an object by using a plane-contact between human fingertip and the object. In terms of above, recently a lot of researches associated with the grasping using a soft fingertip have been studied. Nguyen *et al.* [1] have proposed a simple deformation model of a soft fingertip in order to use analytical mechanics theory in control. But that deformation model assumes that all the elastic forces exerted on the soft fingertip face toward the origin of the fingertip. Therefore, that model cannot derive an local minimum of an elastic potential energy due to the deformation of the soft fingertip, which is represented in this paper. Shimoga *et al.* [2], [3] have conducted an impact experiment so as to decide a best material for the soft fingertip. That paper concluded that a gel tip is most suitable for the soft fingertip by evaluating both of impact and strain energy dissipations quantitatively. Xydas *et al.* [4], [5] have proposed a power law, in which a sectional area of the soft fingertip is related to an normal force caused by normal deformation of the soft fingertip. The Von Mises stress and the strain tensor have been introduced for derivation of the above law. But these techniques as theory of plasticity are so complicated to represent the behavior of the grasped object. Our objective is not to derive an exact deformation model of the soft contact, but a simple static model suitable for stability analysis and deriving equations

of motion of the grasped object.

Inoue *et al.* [6], [7] have proposed three contact models between a soft fingertip and a rigid object: translational contact, rotational contact, and elastic rolling contact models. In this paper, we represent an elastic potential energy due to the deformation of a hemispherical soft fingertip, and newly indicate a local minimum of the potential energy. Also, it is verified that the elastic force and the potential energy are functions of two variables: the maximum displacement of the fingertip and the orientation angle of the contact object.

## II. TRANSLATIONAL CONTACT MODEL

### A. Total Elastic Force on Soft Fingertip

The total elastic force and the potential energy that appear on the entire deformed part of the fingertip is mentioned in this section.

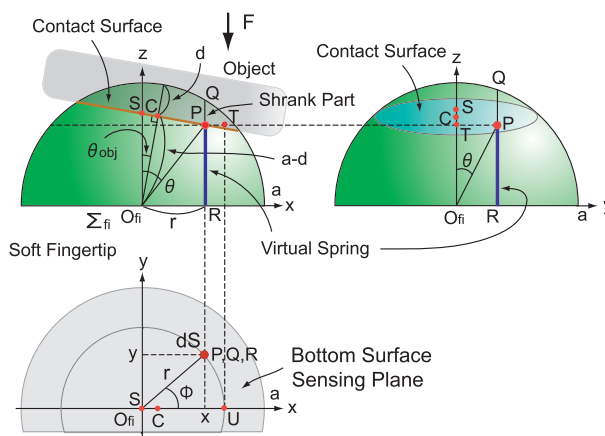


Fig. 1. Translational contact model

As shown in Fig.1, let  $d$  be the maximum displacement, and  $a$  be the radius of the fingertip. Let  $\Sigma_{fi}$  be the fingertip coordinate system,  $O_{fi}$  be the origin of  $\Sigma_{fi}$  coordinate system, and  $R$  be the arbitrary point on  $xy$ -plane of  $\Sigma_{fi}$  coordinate system. Let us introduce a virtual spring on point  $R$  perpendicular to  $xy$ -plane, which has an infinitesimal sectional area  $dS$ . Let  $Q$  and  $P$  be the upper ends of the spring in a natural state and after deformation, respectively. An infinitesimal elastic force appears on the single virtual

spring in the translational contact is then formulated as the following equation [6]:

$$dF(x, y, d, \theta_{obj}) = E\varepsilon(x, y, d, \theta_{obj})dS, \quad (1)$$

where

$$\varepsilon(x, y, d, \theta_{obj}) = 1 - \frac{a - d - x \cdot \sin \theta_{obj}}{\cos \theta_{obj} \sqrt{a^2 - (x^2 + y^2)}}. \quad (2)$$

Note that the symbol  $E$  means Young's modulus and eq.(2) indicates a physical quantity that corresponds to a strain. Since eq.(1) satisfies Hooke's law, the derived force equation is based on mechanics of materials. Furthermore, the symbol  $dF(x, y, d, \theta_{obj})$  represents that the infinitesimal elastic force is a function of four variables  $x, y, d$ , and  $\theta_{obj}$ .

Next, by performing the double integration associated with the elastic force equation, eq.(1), with respect to  $x$  and  $y$ , we can derive the total elastic force equation. In consideration of an orthogonal projection of the contact surface onto  $xy$ -plane shown in Fig.2, the integration area  $S$  is an ellipse on  $xy$ -plane. Let  $A$  and  $B$  be the intersection points between the elliptic curve and  $x$ -axis,  $C$  and  $D$  be the end-points of the elliptic curve along  $y$ -axis, and  $b(x)$  be the  $y$ -coordinate on the boundary of the elliptic curve with respect to  $x$ . A double integration formula of the elastic force with respect to  $x$  and  $y$  is then obtained as below:

$$\begin{aligned} F(d, \theta_{obj}) \\ = E \int_A^B \int_{-b(x)}^{b(x)} \left\{ 1 - \frac{a - d - x \cdot \sin \theta_{obj}}{\cos \theta_{obj} \sqrt{a^2 - (x^2 + y^2)}} \right\} dy dx, \end{aligned} \quad (3)$$

where

$$A = (a - d) \sin \theta_{obj} - \sqrt{a^2 - (a - d)^2} \cos \theta_{obj}, \quad (4)$$

$$B = (a - d) \sin \theta_{obj} + \sqrt{a^2 - (a - d)^2} \cos \theta_{obj}, \quad (5)$$

$$b(x) = \sqrt{a^2 - (a - d)^2 - \frac{\{x - (a - d) \sin \theta_{obj}\}^2}{\cos^2 \theta_{obj}}} \quad (6)$$

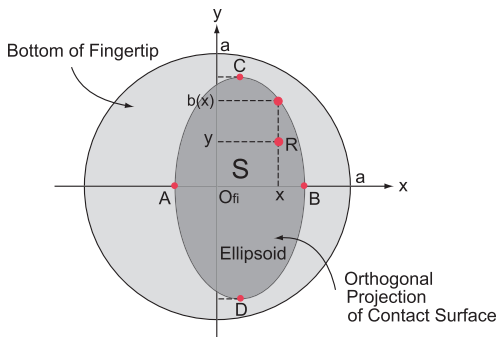


Fig. 2. Integration area

The total elastic force generated on the entire deformed part of the fingertip due to the contact with an object is a function that has two variables of the maximum displacement  $d$  and the object orientation  $\theta_{obj}$ .

### B. Elastic Potential Energy

Let us formulate an elastic potential energy of the shrank part of the fingertip from the translational contact model represented as eq.(1). Let  $k$  be the virtual spring constant and  $PQ$  be the shrinkage of the single virtual spring  $QR$  [6]. The infinitesimal elastic potential energy due to the shrinkage  $PQ$  is then described as follows:

$$dU(x, y, d, \theta_{obj}) = \frac{1}{2}k \cdot PQ^2 = \frac{1}{2}E\lambda(x, y, d, \theta_{obj})dS, \quad (7)$$

where

$$k = \frac{EdS}{\sqrt{a^2 - (x^2 + y^2)}}, \quad (8)$$

$$\begin{aligned} \lambda(x, y, d, \theta_{obj}) &= \sqrt{a^2 - (x^2 + y^2)} - 2 \frac{a - d - x \cdot \sin \theta_{obj}}{\cos \theta_{obj}} \\ &+ \frac{(a - d - x \cdot \sin \theta_{obj})^2}{\cos^2 \theta_{obj} \sqrt{a^2 - (x^2 + y^2)}}. \end{aligned} \quad (9)$$

Therefore, performing the double integration within the elliptic integration area with respect to  $x$  and  $y$ , the total elastic potential energy can finally be written by

$$U(d, \theta_{obj}) = \frac{1}{2}E \int_A^B \int_{-f(x)}^{f(x)} \lambda(x, y, d, \theta_{obj}) dy dx. \quad (10)$$

Next, let us calculate the potential energy analytically in a particular case. When the orientation angle  $\theta_{obj}$  takes zero, which means that the contacting surface of the object is parallel to the bottom surface of the fingertip, the total elastic potential energy is calculated from eq.(10) and Fig.1 as below:

$$U(d, 0) = \frac{1}{2}E \int_B^A \int_{-f(x)}^{f(x)} \lambda(x, y, d, 0) dy dx = \frac{1}{3}\pi Ed^3. \quad (11)$$

The above calculation is detailed in APPENDIX I. As is clear from eq.(11), the total elastic potential energy on the whole deformed part is proportional to the cube of the maximum displacement  $d$  in this case.

## III. SIMULATION

### A. Measurement of Young's Modulus

Since soft materials such as rubber are able to deform largely and easily when these materials are stretched. Also, the sectional area of the specimen decreases readily according to the tension. Therefore, the true stress is used during estimating Young's modulus in a tension test instead of the nominal stress. In this test, a polyurethane specimen that is made simultaneously as a hemispherical soft fingertip is used. Its dimension is approximately  $9\text{mm}^2$  as the sectional area, and the multiple specimens that have each different length have been prepared.

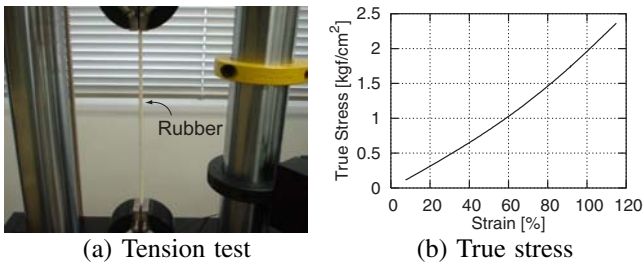


Fig. 3. Measurement of Young's modulus

Fig.3-(a) shows an appearance of the tension test, and Fig.3-(b) represents a stress-strain diagram, in which a slight nonlinearity in terms of the slope of the curve can be seen. That is, Young's modulus, which corresponds to the slope, takes comparatively small value unless the fingertip deforms largely. On the contrary, Young's modulus takes comparatively large value when the fingertip deforms a little. TABLE I shows calculation results using measured true stress plotted in Fig.3-(b). Considering that the deformation of the soft fingertip due to the compression in actual contact process is substantially large, the maximum value of Young's modulus, 0.304MPa, should be adopted as a constant value by computing from the stress-strain diagram.

TABLE I  
YOUNG'S MODULUS

Strain [%]	Young's modulus [MPa]
Min	0.135
20	0.149
40	0.182
60	0.201
80	0.207
100	0.255
Max	0.304

### B. Local Minimum of Elastic Potential Energy

Since it is difficult to calculate the double integration of the elastic force and the potential energy equations analytically, eqs.(3) and (10), we perform the numerical computation of both equations. Fig.4-(a) shows simulation results, in which the object orientation varies from  $-25\text{deg}$  to  $25\text{deg}$ . Four lines correspond to different maximum displacements: 2.0mm, 4.0mm, 6.0mm, and 8.0mm. In this simulation, the radius of the soft fingertip is 20mm, which is equal to the radius of an actual soft fingertip fabricated for this experiment. In addition, the total elastic forces for each different orientation angle that varies from  $0\text{deg}$  to  $30\text{deg}$  are plotted in Fig.4-(b) according to the maximum displacement  $d$ .

Fig.4-(a) shows that the total elastic force reaches to its minimum at angle  $0\text{deg}$ . The rate of change of the force increases as the maximum displacement  $d$  increases. As shown in Fig.4-(b), we see that the elastic force satisfies

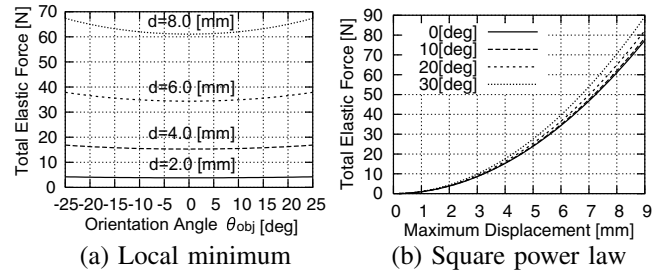


Fig. 4. Total elastic force

a certain power law associated with the maximum displacement. Since the continuous line corresponds to  $\pi Ed^2$  [6], all the curves except  $0\text{deg}$  satisfy a power law whose exponential number is more than the square. Similar results had been shown in a contact experiment of human finger with several experimental subjects [8].

Next, by performing the numerical double integration with respect to  $x$  and  $y$ , the potential energy is obtained, as shown in Fig.5. Several parameters and the horizontal axes in both figures are identical to those in the results of the total elastic force. The vertical axis denotes an elastic potential energy due to the entire deformed part of the fingertip. It is also clearly shown that the local minimum of the potential energy can be seen at  $\theta_{obj} = 0\text{deg}$ . As well as the result of the total elastic force, the rate of change of the potential energy increases as the maximum displacement  $d$  goes up to 8mm. This means that the grasped object by two fingered hand may quickly converge to an equilibrium point, which corresponds to  $\theta_{obj} = 0\text{deg}$ , when the maximum displacement takes a large value in an actual manipulation process. This result indicates that the local minimum of the elastic potential energy will play a substantially important role in realizing stable grasping and manipulation of an object with a soft fingertip.

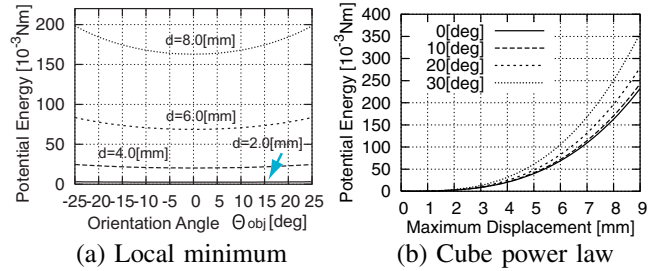


Fig. 5. Elastic potential energy

The potential energy of the continuous line in Fig.5-(b) is proportional to the cube of the maximum displacement  $d$ , as previously shown in eq.(11). Therefore, the relationship between the potential energy and the displacement  $d$  satisfies a power law that exceeds the cube, as the orientation angle increases to  $30\text{deg}$ .

## IV. EXPERIMENTS

### A. Translational Contact Experiment

In this study, a compression test of a hemispherical soft fingertip is performed to compare the derived contact model with experiments. We use a pressure sensor underlaid at the bottom surface of the fingertip. The total force can be computed by summing all pressure values measured by the sensor. The fact that the total elastic force, eq.(3), is a function of the maximum displacement  $d$  and the object orientation  $\theta_{obj}$  is verified in this experiment.

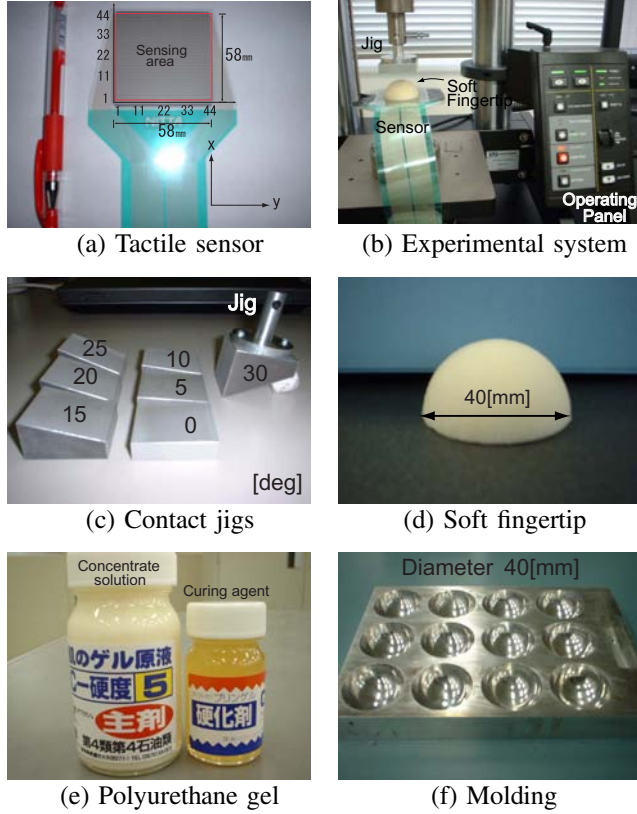


Fig. 6. Setup and tools

1) *Apparatus*: we use a high performance tactile sensor (NITTA Corp.) to measure a pressure value, which is used for the elastic force on the fingertip by multiplying the sensing area of the sensor, as shown in Fig.6-(a). The sensing area of the sensor is approximately 58mm×58mm and has 44×44 sensing points (abbreviated as "cell"). Scanning time for 44×44 cells is about 40msec.

Furthermore, we use a tension test machine that is available for both tension and compression tests, as shown in Fig.6-(b). In this experiment, we alter the maximum displacement  $d$  up to approximately 8mm at a certain orientation angle at intervals of 5deg of the object, as shown in Fig.6-(c). The hemispherical soft fingertip, whose diameter is 40mm, is made by adding curing agent to concentrate solution, and by pouring the compound liquid

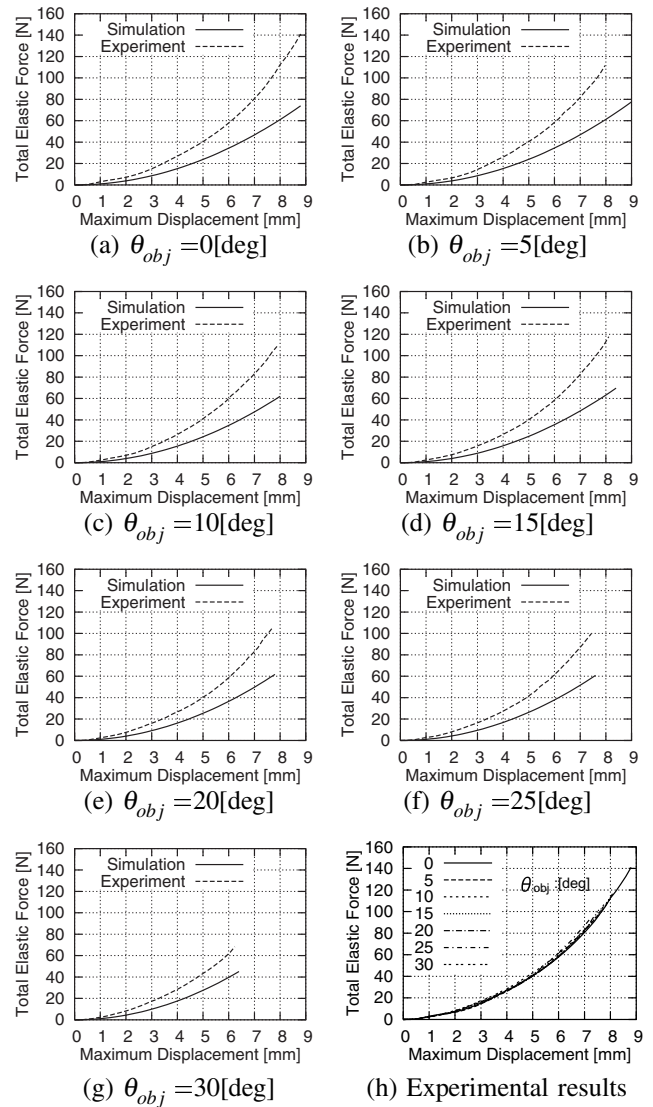


Fig. 7. Simulation and experimental results

into an aluminum molding and being hardened, as shown in Fig.6-(d),(e), and (f).

2) *Experimental Results*: Fig.7 shows experimental results plotted with the simulation results. The orientation angle of the object that varies from 0deg to 30deg corresponds to the counterclockwise of  $\theta_{obj}$  in Fig.1. That is, the apparatus, on which the jigs are mounted, is activated toward vertical direction for the sensing surface as shown in Fig.6-(b). The horizontal and vertical axes denote the maximum displacement and the total elastic force appears on the entire deformed part, respectively.

An approximative constant error between the experimental result and the simulation result has appeared in every figure. By adopting the stress of the narrowed part of the specimen, Young's modulus goes to increase and the simulation result will be close to the experimental result. However, since it is impossible to measure the sectional

area by using a vernier caliper and a micrometer, the stress at the narrowed part is not employed in this study.

Additionally, all experimental results are plotted in Fig.7-(h), in which a similar result compared with the simulation result shown in Fig.4-(b) is obtained. That is, the elastic force of the entire deformed part of the fingertip slightly increases as the orientation angle  $\theta_{obj}$  goes up. Therefore, it is shown that the elastic force is also proportional to the over-square of the maximum displacement  $d$  even in experiments.

### B. Rotational and Rolling Contact Experiments

1) *Apparatus:* We evaluate the elastic force appears on the bottom surface of the soft fingertip as shown in Fig.8. First, we hold the finger on the condition that the soft fingertip contacts with a fixed object keeping parallel along the finger. The finger is tilted up to 11.5deg toward clockwise around the root of the finger with the fixed object. Continuously, The finger is fixed and the object rolls on the fingertip up to 20.7deg toward clockwise rotation. Therefore, the final relative angle of the contact object with respect to  $\Sigma_{fi}$  coordinate system becomes 9.2deg toward clockwise rotation.

In order to compare with experiments, an apparatus is fabricated as shown in Fig.9, which is contrived so that the finger rotates around a central axis in stead of the object rolling on the soft fingertip.

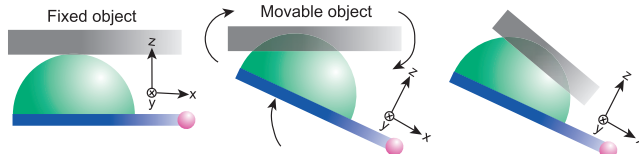


Fig. 8. Pattern diagram for simulation

2) *Experimental Results:* The experimental results are shown in Fig.10, in which the horizontal axis denotes the relative orientation angle with respect to  $\Sigma_{fi}$  coordinate system and the negative sign means the counterclockwise rotation shown in Fig.8. The vertical axis denotes the measured force value from the tactile sensor.

As shown in Fig.10-(a), both paths of the elastic forces of simulation and experimental results in terms of the rotational contact are approximately equivalent to each other. A relatively large error, approximately 17%, have occurred in the elastic rolling contact, as shown in Fig.10-(b). We see that this result is attributed to the fact that the spring constant gets increase according to the deformation in the case of soft materials. Additionally, this result depends on the measurement method of Young's modulus. However, the most important point is that the local minimum of the elastic force appeared as well as the simulation result. Furthermore, the elastic force got to the local minimum slightly before 0deg. We infer that this phenomenon comes

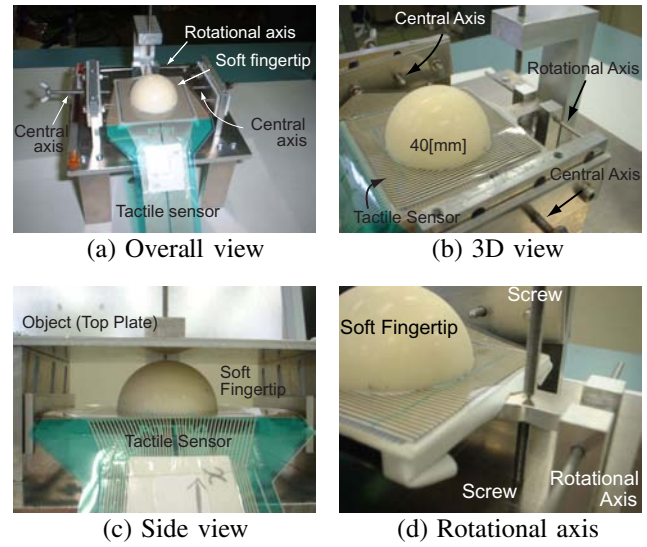


Fig. 9. Apparatus for experiments

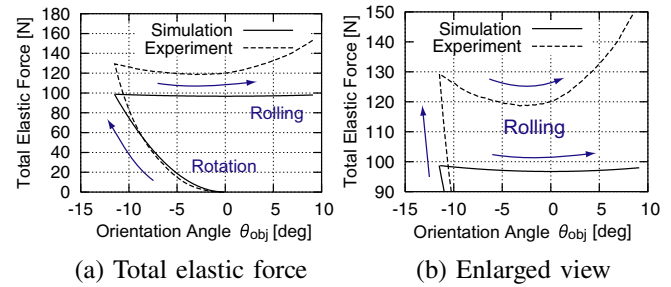


Fig. 10. Total elastic force in rotational and rolling contact

from the strain energy due to the elasticity of the soft fingertip and the potential energy relating to lateral spring components inside the soft fingertip.

### V. CONCLUSION

In this paper, we have developed our contact models and focused on the elastic force and its potential energy required for an actual robotic soft-fingered manipulation. We have firstly shown in a theoretical way that the elastic force and the potential energy due to the shrinkage of the soft fingertip are functions of the maximum displacement of the hemispherical soft fingertip and the orientation angle of the contact object. In a particular case of the orientation angle of an object, we have derived that the potential energy is proportional to the cube of the maximum displacement of a soft fingertip. Furthermore, we have presented in a theoretical sense that the potential energy have a local minimum during the elastic rolling contact, and also obtained similar results in experiments. We infer that the existence of the local minimum of the elastic force allows us to stably grasp and manipulate an object by means of soft fingertips with an easy control law.

In the future, we will derive equations of motion of a

grasped object by two rotational fingers using the concept of the local minimum of the elastic potential energy, and also discuss a quasi-static manipulation.

#### APPENDIX I CALCULATION OF POTENTIAL ENERGY

First, let us convert eq.(10) to an expression in the spherical coordinates.

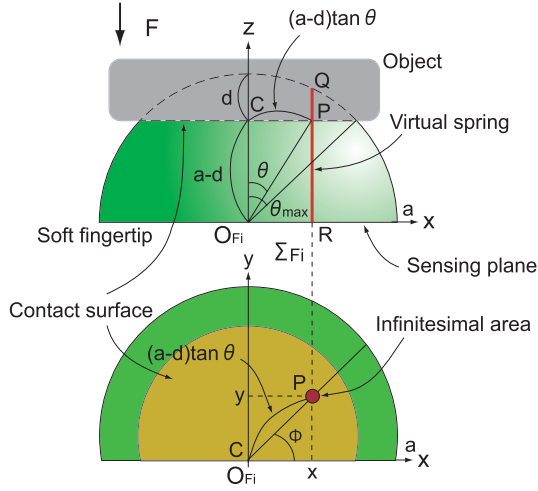


Fig. 11. Translational contact model

As shown in Fig.11, the integration area is transformed into a circle when the orientation angle takes zero. Let  $\theta_{max}$  be the limit angle relating to the contact surface,  $\phi$  be the azimuthal angle on the  $xy$ -plane. The equation (10) can be rewritten by

$$U(d,0) = \frac{1}{2}(a-d)^2 E \int_0^{2\pi} \int_0^{\theta_{max}} \left\{ \sqrt{a^2 - (a-d)^2 \tan^2 \theta} - 2(a-d) + \frac{(a-d)^2}{\sqrt{a^2 - (a-d)^2 \tan^2 \theta}} \right\} \frac{\sin \theta}{\cos^3 \theta} d\theta d\phi, \quad (12)$$

where

$$x^2 + y^2 = (a-d)^2 \tan^2 \theta, \quad (13)$$

$$dxdy = (a-d)^2 \frac{\sin \theta}{\cos^3 \theta} d\theta d\phi, \quad (14)$$

$$\tan^2 \theta_{max} = \frac{a^2 - (a-d)^2}{(a-d)^2}. \quad (15)$$

Let us calculate the first term of the right hand side of eq.(12).

$$\begin{aligned} & \int_0^{2\pi} \int_0^{\theta_{max}} \frac{\sin \theta \sqrt{a^2 - (a-d)^2 \tan^2 \theta}}{\cos^3 \theta} d\theta d\phi \\ &= -\frac{2\pi a^3}{(a-d)^2} \int_{\pi/2}^p \sin^2 t \cos t dt \\ &= \frac{2\pi d}{3(a-d)^2} (3a^2 - 3ad + d^2), \end{aligned} \quad (16)$$

where

$$p = \cos^{-1} \left( \frac{a-d}{a} \tan \theta_{max} \right) = \frac{\pi}{2} - \theta_{max}, \quad (17)$$

Next, let us calculate the second term of the right hand side of eq.(12).

$$\begin{aligned} & \int_0^{2\pi} \int_0^{\theta_{max}} \frac{\sin \theta}{\cos^3 \theta} d\theta d\phi \\ &= -2\pi \int_1^{\cos \theta_{max}} \frac{1}{t^3} dt = 2\pi \int_{\cos \theta_{max}}^1 t^{-3} = -\pi [t^{-2}]_{\cos \theta_{max}}^1 \\ &= \pi \left( \frac{1}{\cos^2 \theta_{max}} - 1 \right) = \pi \frac{a^2 - (a-d)^2}{(a-d)^2}, \end{aligned} \quad (18)$$

Furthermore, the third term is calculated as below:

$$\begin{aligned} & \int_0^{2\pi} \int_0^{\theta_{max}} \frac{\sin \theta}{\cos^3 \theta \sqrt{a^2 - (a-d)^2 \tan^2 \theta}} d\theta d\phi \\ &= \frac{2\pi d}{(a-d)^2}, \end{aligned} \quad (19)$$

Hence, from eqs.(16),(18) and (19), the equation (10) can finally be represented as the following equation:

$$U(d,0) = \frac{1}{3} \pi E d^3. \quad (20)$$

#### REFERENCES

- [1] P.Nguyen and S.Arimoto, "Performance of Pinching Motions of Two Multi-DOF Robotic Fingers with Soft-Tips", *Proc. IEEE Int. Conf. on Robotics and Automation*, pp.2344-2349, 2001.
- [2] K.Shimoga and A.Goldenberg, "Soft Robotic Fingertips Part I: A Comparison of Construction Materials", *Journal of Robotics Research*, Vol.15, No.4, pp.320-334, 1996.
- [3] K.Shimoga and A.Goldenberg, "Soft Robotic Fingertips Part I I : Modeling and Impedance Regulation", *Journal of Robotics Research*, Vol.15, No.4, pp.335-350, 1996.
- [4] N.Xydas and I.Kao, "Modeling of Contact Mechanics and Friction Limit Surfaces for Soft Fingers in Robotics, with Experimental Results", *Journal of Robotics Research*, Vol.18, No.8, pp.941-950, 1999.
- [5] N.Xydas, M.Bhagavat, and I.Kao, "Study of Soft-Finger Contact Mechanics Using Finite Elements Analysis and Experiments", *Proc. IEEE Int. Conf. on Robotics and Automation*, pp.2179-2184, 2000.
- [6] T.Inoue and S.Hirai, "Modeling of Soft Fingertip for Object Manipulation Using Tactile Sensing", *Proc. IEEE Int. Conf. on Intelligent Robots and Systems*, pp.2654-2659, 2003.
- [7] T.Inoue and S.Hirai, "Rotational Contact Model of Soft Fingertip for Tactile Sensing", *Proc. IEEE Int. Conf. on Robotics and Automation*, pp.2957-2962, 2004.
- [8] H.Han and S.Kawamura, "Analysis of Stiffness of Human Fingertip and Comparison with Artificial Fingers", *Proc. IEEE Int. Conf. on Systems, Man, and Cybernetics*, pp.800-805, 1999.